Check for updates

View Article Online
View Journal

Journal of
Materials Chemistry A

Materials for energy and sustainability

Accepted Manuscript

This article can be cited before page numbers have been issued, to do this please use: M. J. Clark, D. N. Rainer, J. Yang, S. J. Coles, D. Bradshaw and A. M. Nightingale, *J. Mater. Chem. A*, 2026, DOI: 10.1039/D6TA03191A.


This is an Accepted Manuscript, which has been through the Royal Society of Chemistry peer review process and has been accepted for publication.

Accepted Manuscripts are published online shortly after acceptance, before technical editing, formatting and proof reading. Using this free service, authors can make their results available to the community, in citable form, before we publish the edited article. We will replace this Accepted Manuscript with the edited and formatted Advance Article as soon as it is available.

You can find more information about Accepted Manuscripts in the Information for Authors.

Please note that technical editing may introduce minor changes to the text and/or graphics, which may alter content. The journal's standard Terms & Conditions and the Ethical guidelines still apply. In no event shall the Royal Society of Chemistry be held responsible for any errors or omissions in this Accepted Manuscript or any consequences arising from the use of any information it contains.

ROYAL SOCIETY OF CHEMISTRY

rsc.li/materials-a

# Application-led, online analysis of flow synthesised Metal-Organic Frameworks (MOFs)

View Article Online
DOI: 10.1039/D6TA03191A

Molly J. Clark,[a,b] Daniel N. Rainer,[b] Josiah Yang,[a] Simon J. Coles,[b] Darren Bradshaw,[b] and Adrian M. Nightingale.[a]

[a] Mechanical Engineering Department, School of Engineering, Faculty of Engineering and Physical Sciences, University of Southampton, Southampton, SO17 1BJ, United Kingdom.

[b] School of Chemistry & Chemical Engineering, Faculty of Engineering and Physical Sciences, University of Southampton, Southampton, SO17 1BJ, United Kingdom.

Open Access Article. Published on 23 June 2026. Downloaded on 6/24/2026 4:50:44 AM.
This article is licensed under a Creative Commons Attribution 3.0 Unported Licence.

## ABSTRACT

Metal organic frameworks (MOFs) have numerous important large-scale industrial applications such as gas storage, energy storage, and water purification and remediation. The prospect of industrial usage means there is a need to develop efficient processes for scalable quality-assured MOF production. Flow reactors offer a promising route to scalable MOF synthesis. They feature high space-time-yields, easy automation and reduced manual handling, however quality assurance is challenging: the standard MOF analysis methods (X-ray diffraction, electron microscopy, gas adsorption etc) are slow, costly, and manually intensive, and hence difficult to apply to production scenarios. Here we present an alternative approach to MOF analysis that is quick, easily automated, and can be implemented into flow reactors for continuous assessment of flow-synthesised MOFs. Rather than look to the standard MOF characterisation methods, we developed an "application-led" quantitative test that mimicked an example end application – water remediation – by testing how well the reaction product could remove an organic dye from solution. The method was integrated into a flow reactor making HKUST-1 MOF and used to continuously monitor the reactor output (0.67 Hz frequency) in near real-time (22.4 min lag). It could clearly differentiate product made under different reaction conditions (most notably reaction stoichiometry) with the amount of dye removed corresponding to the composition of the product (HKUST-1 versus unwanted side-product). The product could be assessed "on-the-fly", with changes in product continuously tracked as reaction conditions were systematically altered. This work will be a starting point for other application-led online analysis methods and, if combined with computer-controlled flow reactors opens the way to rapid automated exploration of MOF reaction space.

Journal of Materials Chemistry A Accepted Manuscript

View Article Online
DOI: 10.1039/D6TA03191A

Open Access Article. Published on 23 June 2026. Downloaded on 6/24/2026 4:50:44 AM.
This article is licensed under a Creative Commons Attribution 3.0 Unported Licence.

Journal of Materials Chemistry A Accepted Manuscript

## INTRODUCTION/BACKGROUND

Metal organic frameworks (MOFs) are self-organising crystalline materials formed when organic linker molecules connect *via* metal nodes to make extended ordered three-dimensional networks.[1, 2] MOFs typically feature large pore sizes giving them exceptionally large specific surface areas.[3] When combined with the tunability of MOF structure, *via* linker and metal choice,[4] this means MOFs have an exceptionally wide range of potential structures, functionality, and hence applications, including molecular separation,[5] catalysis,[6] drug delivery,[7] sensing,[8] and water remediation.[9]

MOFs can be readily synthesised by various methods including solvothermal,[10] microwave-assisted,[11] electrochemical,[12] mechanochemical,[13] and chemical vapour deposition,[14] however recent advances have shown that flow synthesis can produce MOFs with exceptional levels of efficiency and throughput,[15, 16] with the highest reported space-time-yields for MOFs having been *via* flow synthesis.[15] Flow synthesis involves the continuous introduction of reagents into a reactor manifold where they mix and react to yield a stream of product. Different chemical processes, such as multiple reaction stages, work-up, and purification can be concatenated into a single process stream, allowing integrated automated production with reduced manual handling.[17, 18] Larger quantities can be made by running for longer times or by running several reactors in parallel[19] (thus increasing output without changing overall process chemistry), making flow reactors highly suitable for small to medium scale production.

One of the key advantages of flow synthesis is the ability to use inline analysis (where the reaction stream is probed non-invasively) or online analysis (whereby samples are autonomously taken and analysed) to monitor reaction progress and assess product quality in real-time.[20] This vastly increases reactor utility, not only allowing quality-assured production but also enabling high-throughput reaction space exploration[21, 22] and algorithm-driven reaction optimisation.[23-26] While many different inline and online analysis methods have been used with flow synthesis (e.g. inline IR, NMR, optical absorbance and fluorescence, and online chromatographic methods[27, 28]) inline and online analysis of MOFs is challenging. The standard MOF characterisation techniques (e.g. X-ray diffraction, electron microscopy, gas adsorption) are intrinsically offline due to equipment size, cost, manual operation, and measurement duration and hence difficult to translate to an equivalent inline or online analysis method. The few reports describing inline analysis of MOFs feature flow synthesis at synchrotron beamlines[29, 30] to study crystallisation *in situ* using high-power X-ray diffraction. While effective, this is not an option for routine industrial or laboratory synthesis and there remains a need for accessible inline or online analysis methods.

Here we describe a method for online analysis of MOFs that can be routinely implemented in flow synthesis. Instead of looking to implement the typical MOF characterisation techniques (X-ray diffraction, gas adsorption etc), we use an alternative approach: devising a quantitative test based on an end-use application. This approach looks to determine the "fitness" of the product to perform the target application rather than directly measure its physicochemical properties. To showcase this approach we describe the flow-synthesis and analysis of exemplar MOF HKUST-1 [$Cu_3(BTC)_2(H_2O)_3$] (where BTC = 1,3,5-benzenetricarboxylate), which is synthetically and structurally well understood. We introduce an online analysis method, inspired by MOF use for water remediation,[31-33] which quantifies the newly-synthesised framework's ability to remove organic molecules from solution. We show how this method could successfully assess product quality in near real-time and differentiate between favourable and non-favourable reaction conditions.

View Article Online
DOI: 10.1039/D6TA03191A

## RESULTS

The experimental set up (Fig. 1 and image in ESI Fig. S1) combined flow synthesis and online analysis modules. The synthesis stage comprised a simple two-reagent room temperature reaction whereby syringe pumps drove the framework-forming metal salt ($Cu^{2+}$) and BTC linker into a T-junction, from which they mixed and reacted as they flowed downstream through fused silica capillary tubing (10 m, inner diameter 0.7 mm) with a residence time of 10 - 50 min depending on total flow rate. From the synthesis module, the reaction mixture could be directly obtained or routed into the online analysis module. The analysis module was composed of three sub-sections: firstly an initial dye incubation stage (Fig. 1, A) where an organic dye (methylene blue) was introduced to the product stream and allowed to mix and adsorb to the MOF reaction product, present as a suspended solid. Subsequently, a separation stage (Fig. 1, B) removed unadsorbed (free) dye from the stream and quantified it *via* optical absorbance (Fig. 1, C). This determined the amount of free dye – and hence the amount of dye adsorbed by the reaction product.

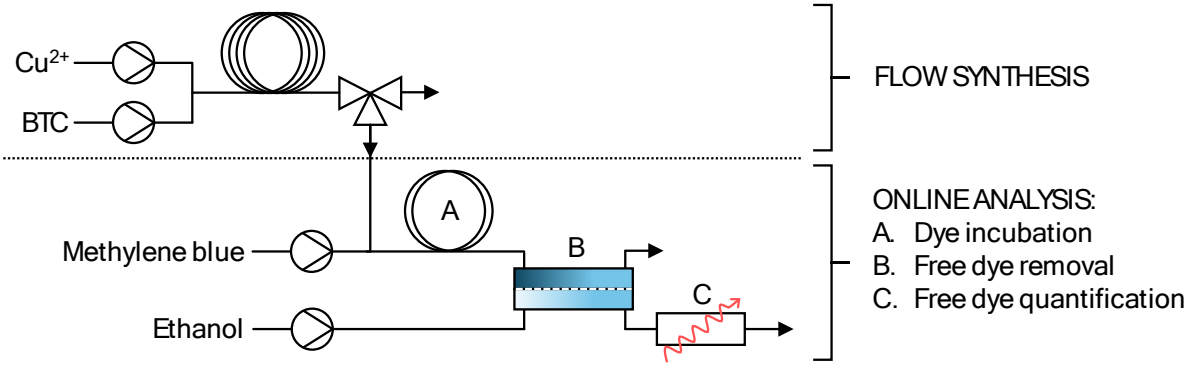


*Figure 1: Schematic illustrating the experimental setup, combining flow synthesis of HKUST-1 (top) with online analysis (bottom) testing the product's ability to adsorb an exemplar organic dye. During online analysis methylene blue is added and incubated (A), unadsorbed dye removed by cross-flow filtration (B) and then quantified using UV-Vis spectrometry (C).*

Initial testing focussed on the flow synthesis in isolation to establish appropriate reaction conditions for HKUST-1 formation in this reactor. Both reactor residence time ($t_{res}$) and metal:linker ratio (M:L) had notable effects on the quantity and phase purity of the MOF product. For all M:L values, increasing $t_{res}$ (by decreasing total flow rate) up to $t_{res}$ = 40 min steadily increased the amount of product per unit volume of reaction mixture, with minimal increases thereafter (Fig. 2a). When stoichiometry was varied, M:L values at 1:2 gave maximum yield, decreasing as stoichiometry became progressively more metal- or linker-rich. It should be noted that while longer residence times gave more product per unit volume of reaction mixture (which will give greater efficiency as determined by green chemistry metrics such as E-factor) the accompanying reduced flow rates results in reduced space-time yields (STYs): STYs for M:L = 1:2 were 137 $kg.m^3.day^{-1}$ at $t_{res}$ = 10 mins, decreasing to 53 $kg.m^3.day^{-1}$ at $t_{res}$ = 40 mins. These values are at the lower end of previous literature values (which range from 10s to 1000s $kg.m^3.day^{-1}$)[34] and is commensurate with the fact that the synthesis was not optimised for STY, with reaction temperatures lower - and reagent loadings up to an order of magnitude lower - than previous flow syntheses of HKUST-1.[34-37]

Offline PXRD analysis confirmed the presence of crystalline products (Fig. 2b,c) with sharper diffractograms obtained at longer reaction times - indicative of the formation of larger crystallites (compare e.g. Fig. 2b, $t_{res}$ = 40 min, *vs* Fig. 2c, $t_{res}$ = 20 min). While all diffraction patterns featured coincident peaks with the HKUST-1 reference spectra, additional peaks (e.g. at 2θ = 8° and 28°) were evident under linker-rich synthesis conditions (most notably

Open Access Article. Published on 23 June 2026. Downloaded on 6/24/2026 4:50:44 AM.
This article is licensed under a Creative Commons Attribution 3.0 Unported Licence.

Journal of Materials Chemistry A Accepted Manuscript

View Article Online
DOI: 10.1039/D6TA03191A

where M:L = 1:4 or 1:8) and were also more pronounced at lower reaction times (Fig. 2c). These peaks are consistent with the presence of an additional crystalline phase.

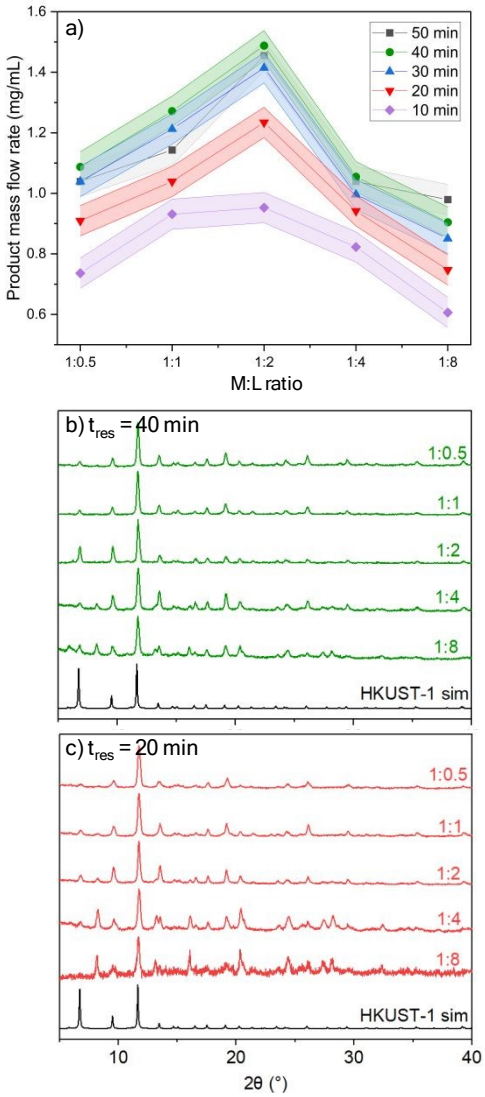


*Figure 2: Results from the reaction module in isolation. a) Graph showing how reaction product output varied with metal:linker ratio (M:L) and residence time ($t_{res}$), with maximum product at a M:L = 1:2 and at longer $t_{res}$ values. Shaded region indicates the standard deviation from repeated measurements. b) & c) PXRD patterns of HKUST-1 synthesised using different M:L ratios at $t_{res}$ = 40 min (b) and 20 min (c).*

The product samples were then examined using scanning electron microscopy (SEM). In samples where the PXRD patterns closely matched the expected HKUST-1 pattern (e.g. Fig. 3a, M:L = 1:2, $t_{res}$ = 40 min) sub-micron crystals with the typical octahedral morphology[38, 39] were observed. Where the PXRD data featured prominent additional peaks (Fig. 3b, M:L = 1:8, $t_{res}$ = 20 min) the morphology was very different, primarily consisting of elongated crystals with a hexagonal cross section, consistent with the presence of a different product. To identify this product and confirm the identity of the supposed HKUST-1 crystals, 3D electron diffraction (3D ED) was used to probe individual crystals from each sample and determine their crystal structures (Fig. 3c-g).

Open Access Article. Published on 23 June 2026. Downloaded on 6/24/2026 4:50:44 AM.
This article is licensed under a Creative Commons Attribution 3.0 Unported Licence.

Journal of Materials Chemistry A Accepted Manuscript

View Article Online
DOI: 10.1039/D6TA03191A

Open Access Article. Published on 23 June 2026. Downloaded on 6/24/2026 4:50:44 AM.
This article is licensed under a Creative Commons Attribution 3.0 Unported Licence.

Journal of Materials Chemistry A Accepted Manuscript

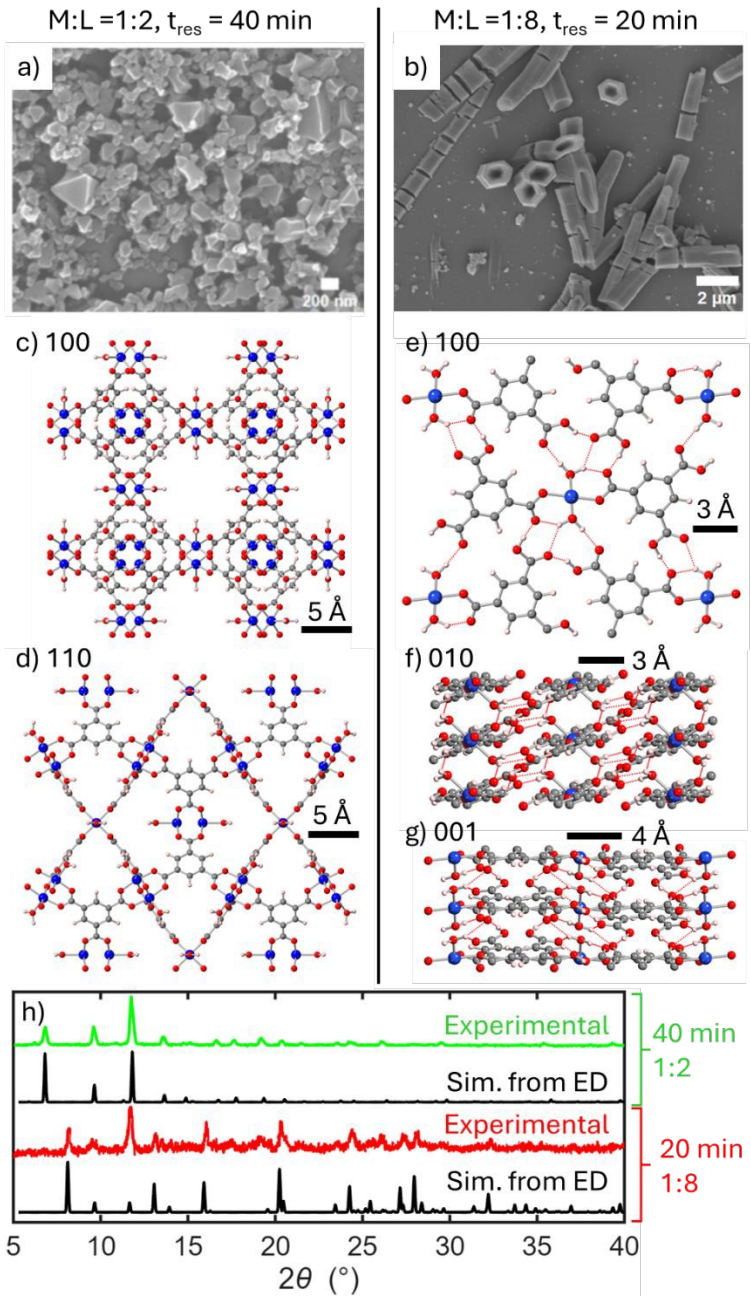


*Figure 3: Scanning electron microscopy images (a & b) of product obtained at M:L and $t_{res}$ values of 1:2, 40 min (a) and 1:8, 20 min (b) respectively. c)-d) crystal unit cell reconstructed from electron diffraction data for product in (a), showing the typical HKUST-1 structure. e)-g) crystal unit cell reconstructed from electron diffraction data for product in (b) showing a condensed non-porous structure. h) Simulated PXRD spectra for the crystal structures in c)-d) and e)-g), shown compared to the experimental spectra obtained from bulk samples.*

The crystal structure from the octahedral crystals obtained at M:L = 1:2, $t_{res}$ = 40 min (Fig. 3c,d) showed the expected HKUST-1 structure with characteristic large pores and twisted boracite topology ($a$=$b$=$c$=25.9 Å, space group $Fm3m$). By contrast, the sample obtained at M:L = 1:8, $t_{res}$ = 20 min (Fig. 3e-g) had a very different and notably non-porous structure ($a$=3.7 Å, $b$=18.3 Å, $c$=13.5 Å, $\beta$ = 91.55 °, space group $P2_1/c$). While these structures were obtained from individual crystals, PXRD fully confirmed that they were representative of the bulk material. Simulated PXRD patterns generated from the 3D ED

View Article Online
DOI: 10.1039/D6TA03191A

derived structures matched exceptionally well with the experimental patterns (Fig 3h), further confirming that these two different reaction conditions favoured very different products.

The 3D ED structures show that the material generated under M:L = 1:8 linker-rich conditions was an extended Cu:BTC coordination polymer with a more ligand-heavy composition (Cu:BTC = 1:2) compared with HKUST-1 (Cu:BTC = 1:0.66), commensurate with the linker-rich formation conditions. In a previous report of this Cu:BTC polymer it was shown that the differing crystal structure resulted in very different material properties compared to the HKUST-1 target phase – most notably a specific surface area (SSA) that was lower by orders-of-magnitude[40] due to the absence of large-volume pores. Hence it is clear that synthesis conditions need to be tightly controlled in this flow reactor to ensure crystalline HKUST-1 is produced and to limit unwanted side-products with inferior properties. Given that this reaction could produce material with different potential compositions, it also therefore provided an excellent opportunity to test whether online application-driven analysis could differentiate between the two potential products and hence determine product quality.

In developing an application-based online analysis method, a suitable application needed to be selected. Water remediation, where the MOF is used as an adsorbent to remove pollutants,[31-33] was chosen as HKUST-1 has been shown to be highly effective for removing organic contaminants[38, 41-44] and could be feasibly translated into an online test. To quantify the product's ability to remove organic molecules from solution, an online test was built around removal of an organic dye as dye concentrations can be easily quantified inline *via* optical methods. Methylene blue was used as the test dye as it has been previously shown to adsorb strongly to HKUST-1,[38, 41, 42] was found in preliminary testing to be soluble in the reaction solvent, stable under ambient conditions, and unaffected by the reaction starting materials.

The adsorption stage (Fig. 1, A) was first tested in isolation by flowing through the dye (0.01 mM in ethanol) with a pre-synthesised suspension of HKUST-1 particles made in a batch reactor (dye and HKUST-1 supplied at a 1:1 volumetric ratio). The HKUST-1 was supplied in its raw reaction mixture (i.e. containing unreacted metal salt and linker molecules) and was diluted inline to give a range of product loadings (Fig. 4a) to test how the amount of HKUST-1 would correlate with dye adsorption. Fig. 4b shows the absorbance spectra of the free dye following incubation, collection, and subsequent removal of the MOF (along with any adsorbed dye) *via* centrifugation. The spectral shape showed minimal change, indicating no chemical change to the dye, and the intensity decreased with increasing HKUST-1 loading as expected due to adsorption of the dye. When the quantity of remaining dye was plotted against loading (Fig. 4c) there was a smooth monotonic relationship, indicating that the amount of adsorbed dye is a good indicator for the amount of HKUST-1 formed.

It should be noted that these measurements were carried out on a raw reaction mixture, confirming that in the final setup (Fig. 1) product could be fed directly from the reaction module into the analysis section without need for work-up. This is advantageous as an additional work up stage would introduce additional complexity and lag-time between reaction and analysis.

Open Access Article. Published on 23 June 2026. Downloaded on 6/24/2026 4:50:44 AM.
This article is licensed under a Creative Commons Attribution 3.0 Unported Licence.

Journal of Materials Chemistry A Accepted Manuscript

View Article Online
DOI: 10.1039/D6TA03191A

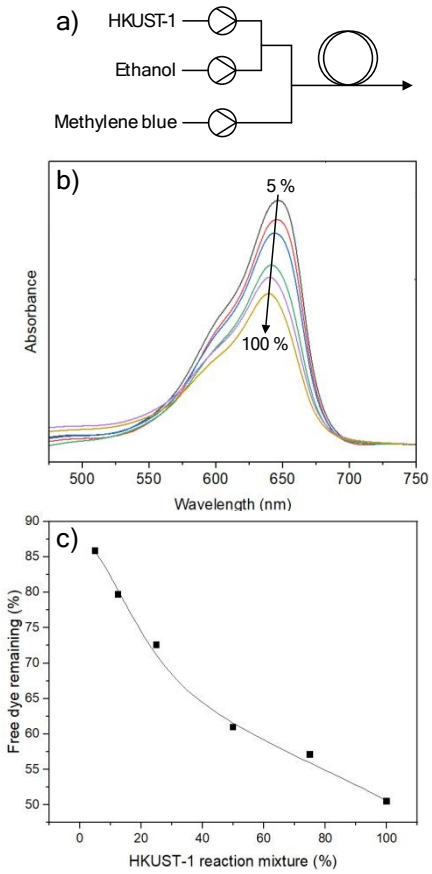


*Figure 4: Results from the dye incubation stage in isolation. a) Experimental setup showing how HKUST-1 reaction mixture was diluted with ethanol inline before dye addition. b) Absorbance spectra of dye solutions after exposure to different dilutions of HKUST-1. Increasing HKUST-1 concentration resulted in a reduced absorbance peak, indicative of a lower concentration of free dye. c) The quantity of free dye in solution, expressed relative to the starting concentration, decreases with HKUST-1 loading in a smooth monotonic relationship.*

The adsorption stage (Fig. 1, A) was finally integrated with both the synthesis module (Fig. 1, top section), and inline dye separation (Fig. 1, B). Inline separation was achieved by cross-flow filtration, with the MOF and dye mixture (donor stream) flowing over a hollow-fibre polyethersulfone (PES) filter membrane, allowing free dye to diffuse across the membrane into an acceptor stream of ethanol flowing on the opposite side. We used a co-flow arrangement (both donor and acceptor streams flowing in the same direction, see Fig. 1, B) which meant a maximum of 50% of free (unadsorbed) dye could be extracted from the donor stream. Counter-flow, where donor and acceptor streams flow in opposite directions, could potentially remove 100% and was initially trialled, however this flow arrangement proved problematic; when operated in counter-flow there was pressure-driven mass transport across the membrane (rather than diffusion-driven transport) due to the pressure drop through the filtration device. This resulted in clogging due to MOF being driven against the filter membrane surface. Using co-flow however, the matched flow direction and flow rates resulted in no pressure difference across the membrane, cross-membrane transport was only diffusion-driven, no clogging was encountered, and all product was recovered.

Open Access Article. Published on 23 June 2026. Downloaded on 6/24/2026 4:50:44 AM.
This article is licensed under a Creative Commons Attribution 3.0 Unported Licence.

Journal of Materials Chemistry A Accepted Manuscript

View Article Online
DOI: 10.1039/D6TA03191A

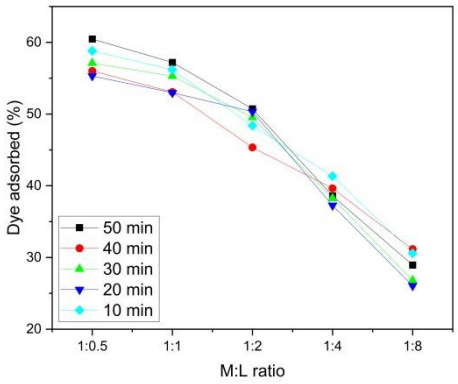


*Figure 5: The amount of dye removed by the reaction product, shown as a function of M:L and $t_{res}$, in the integrated setup combining synthesis and analysis.*

To test the dye adsorption and separation stages in combination with the synthesis stage, we repeated the reaction parameter screening experiment (Fig. 2). The product mass flow rate results were near-identical to those previously observed with product increasing with $t_{res}$ up to 30 min, a maximum yield of 1.5 mg/ml, and a high dependency on stoichiometry: product yield peaking at M:L = 1:2 and decreasing as stoichiometry deviated from this value (ESI Fig. S2). The dye adsorption results showed a strikingly different trend however (Fig. 5). There was a much weaker dependence on residence time and a very different dependency on stoichiometry, with dye adsorption decreasing monotonically as M:L became increasingly linker-rich.

The seeming disparity between the stoichiometry dependency of the product mass flow rate and dye adsorption are explained by considering that the reactor can generate two potential products. The dye adsorption results match well with PXRD results, where the features associated with the non-porous Cu-BTC polymer byproduct (Fig. 2,3) appeared at higher linker content. While we know that HKUST-1 is effective at removing dye (Fig. 4), the non-porous Cu:BTC polymer has much lower SSA,[40] which has been recently shown to correlate with dye adsorption capability.[45] Hence the dye adsorption dependence on stoichiometry is indicative of the different products being produced under different reaction conditions.

We then completed the online analysis setup by adding inline absorbance measurement (Fig. 1, C) to yield the fully integrated flow synthesis and online analysis setup (Fig. 1 and image in ESI Fig. S1) which produced real-time data as the material was being produced. To show how it could be used to track reaction conditions “on-the-fly” we varied M:L ratio (at constant $t_{res}$ = 40 min) whilst monitoring dye removal. The residence time in the analysis module meant that results were obtained 22.4 min after the reaction stream exited the reaction module. The stoichiometry was changed approximately every 15 min, starting with M:L = 1:8, then increasing the metal content stepwise until it reached M:L = 1:0.5. As shown in Fig. 6, the online analysis produced a continuous noise-free signal (measurement rate 0.67 Hz) with clear differentiated responses for each set of reaction conditions and smooth transitions traced in exacting detail. Stable plateaued measurements were obtained after each change of M:L, indicating the stability of both the analytical method and the synthesis conditions. Dye absorption increased with metal content, consistent with earlier results and fully consistent with production of higher quantities of HKUST-1. After the M:L ratio had reached 1:0:5, it was then shifted back towards more ligand-rich conditions, repeating the measurements at M:L = 1:1, 1:2, and 1:4. The repeats closely matched initial results - 52.9 % *vs* 52.7 % for 1:4, 58.8 % *vs* 57.5 % for 1:2, 64.0 % *vs* 63.1 % for 1:1 - showing the reproducibility of the synthesis and online analysis method. Combined with the fine, noise-

Open Access Article. Published on 23 June 2026. Downloaded on 6/24/2026 4:50:44 AM.
This article is licensed under a Creative Commons Attribution 3.0 Unported Licence.

Journal of Materials Chemistry A Accepted Manuscript

View Article Online
DOI: 10.1039/D6TA03191A

free nature of the measurements, this clearly validates the method and shows its ability to assess and track synthesis in near real-time.

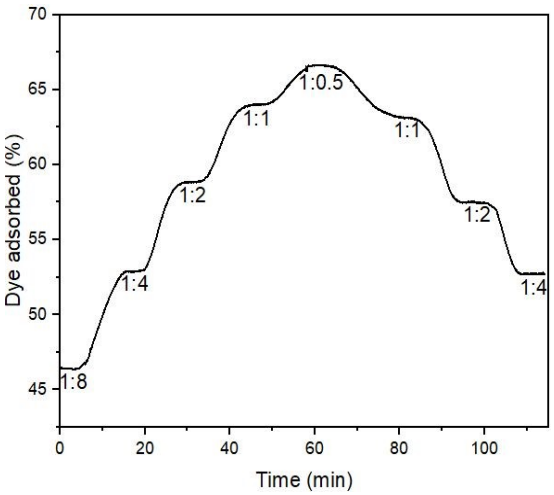


*Figure 6: Real-time online analysis while varying M:L and keeping $t_{res}$ constant at 40 min.*

## DISCUSSION

This work shows how dye adsorption online testing can give near real-time assessment of MOFs continuously produced *via* flow synthesis. This method not only reports on product formation (which could, for example, be measured *via* turbidity[46, 47]) but gives information on the composition of the product, with the ability of the product to remove dye being indicative of the amount of the desired HKUST-1 in the reaction product. While the aim in this work was to create a method that mimicked an end application and not to use dye adsorption specifically as a proxy-surface area measurement, this is in effect what is being done and it is interesting to note that Han *et al.* recently suggested a similar approach for accelerated porosity screening of several porous materials (MOFs, porous organic cages, and conjugated microporous polymers).[45] Unlike their report, however, our measurements are quantitative, fully automated, and significantly more rapid (minutes rather than hours).

Using an application-led approach for online analysis opens up an array of potential methods with the dye adsorption method used here just one possibility. Dye absorption was a direct analogy for an end application of remediating water fouled by organic pollution, however a similar approach could be adopted for other applications. Online analysis methods will be necessarily limited to solution-based protocols (excluding gas-based end-use applications) however that still includes several applications based around solution-based adsorption such as sensing and catalysis. Finally we note that while this approach does not directly characterise physicochemical properties, if the MOF is to be used in - or developed for - a specific application, analytical methods that directly link to that application will be the most pertinent test of product quality.

## CONCLUSION

We have outlined a strategy whereby application-led online testing can be used to get near-real time data of flow-synthesised MOFs. This is the first report, to our knowledge, to show inline or online characterisation of flow synthesised MOFs away from a synchrotron beamline. It opens the way to monitoring MOF quality in production scenarios and could be coupled to computer reaction control to allow high throughput automated exploration of reaction space and/or reaction optimisation.[23, 48, 49]

Open Access Article. Published on 23 June 2026. Downloaded on 6/24/2026 4:50:44 AM.
This article is licensed under a Creative Commons Attribution 3.0 Unported Licence.

Journal of Materials Chemistry A Accepted Manuscript

View Article Online
DOI: 10.1039/D6TA03191A

Open Access Article. Published on 23 June 2026. Downloaded on 6/24/2026 4:50:44 AM.
This article is licensed under a Creative Commons Attribution 3.0 Unported Licence.

Journal of Materials Chemistry A Accepted Manuscript

View Article Online
DOI: 10.1039/D6TA03191A

## METHODS

### *Materials*

All chemicals and reagents were purchased from Sigma Aldrich unless specified. No further purification was necessary. Syringes (20 mL, BD Plastipak Luer Lock) and tubing (PTFE, 1 mm ID) were purchased from RS components. Fused silica capillary (700 µm ID) was purchased from CM Scientific. Fluid was delivered by syringe pumps (Pump 11 OEM, Harvard apparatus) fitted with 20 mL syringes and controlled *via* computer using software developed in-house (LabView). All connectors used were IDEX flangeless ¼-28" fittings.

### *Integrated flow synthesis and online analysis*

In a typical run of the fully integrated inline synthesis and analysis system, two syringe pumps were loaded with syringes containing solutions of copper(II) nitrate hemipentahydrate (98 %, 0.03 M in ethanol) and BTC (95 %, 0.06 M in ethanol). Each syringe was connected *via* PTFE tubing (10 cm, ID = 1 mm) to a T-junction (IDEX) where the reagent streams met and exited into fused silica capillary (10 m, ID = 0.7 mm) that acted as the reaction manifold. Hydrophilic silica tubing was used for the synthesis section because initial tests using hydrophobic PTFE resulted in channel fouling (see ESI Fig. S3). No fouling was observed using silica. MOF did not foul PTFE channel surfaces in the subsequent analysis stages suggesting that fouling during synthesis could be associated with heterogenous MOF nucleation at channel walls.

The exit of the silica capillary was attached to a second T-junction which introduced methylene blue solution (0.01 mM in ethanol). The methylene blue was added at the same flow rate as the combined reagent flow rate to ensure a constant volumetric ratio between the dye solution and the reaction solution. The combined flow subsequently passed through PTFE tubing (4 m, ID = 1 mm). PTFE tubing was used as in initial tests using silica capillary, dye was found to adhere to channel walls. This resulted in a relative residence time of 41 % compared to the residence time in the silica capillary manifold for synthesis. Initial offline testing showed that a minimum of 2 min was required for adsorption with freshly made reaction product (data not shown), meaning that in the integrated system, reaction residence times down to a minimum of 5 min could be tolerated. The process stream exited this section into a Repligen Spectrum MicroKros hollow fibre filter (65 cm length, 9 lumens of 0.5 mm inner diameter, PES membrane material with 0.2 µm pore size, 92 $cm^2$ surface area). The process stream travelled through the exterior, while ethanol (the acceptor stream) travelled through the hollow fibre filters in a co-flow regime at the same flow rate. The dimensions of the filtration device gave a comparative residence time of 15 % compared to the residence time in the silica capillary manifold for synthesis. Initial offline testing showed that an approximate minimum residence time of 1 min was required for the expected 50 % dye removal, which would correspond to a minimum 6.7 min reaction residence time.

After exiting the filtration device, the acceptor stream was directed into a spectrophotometric flow cell to determine the amount of dye that had been removed from the process stream. The flow cell was composed of a 3D-printed structure (designed in-house and printed in black PLA) which housed PTFE tubing (ID 1 mm), through which the acceptor stream flowed, and optical components which directed a spectrum of visible light across the channel. The light came from a halogen lamp (Ocean Optics HL-2000) and was transmitted to the tubing in the flow cell *via* an armoured fibre optic assembly (Ocean Optics INTSMA-200). Light transmitted across the channel was collected into another fibre optic assembly and delivered to a CCD spectrophotometer (Ocean Optics FLAME-S-VIS-NIR-ES). OceanView software (v 2.0) was used to record the spectra, using an integration time of

Open Access Article. Published on 23 June 2026. Downloaded on 6/24/2026 4:50:44 AM.
This article is licensed under a Creative Commons Attribution 3.0 Unported Licence.

Journal of Materials Chemistry A Accepted Manuscript

View Article Online
DOI: 10.1039/D6TA03191A

1500 µs per scan and with 1000 scans averaged to generate each spectrum. The equations used to calculate the quantity of adsorbed dye are given in the ESI. As absorbance measurements require accurate blank measurements, a T junction and on/off valve (IDEX, not shown in Fig. 1) were included upstream of the flow cell, to allow a blank to be flushed through the flow cell periodically. The blank used was the supernatant from an isolated reaction (i.e. with product removed) – mimicking the process stream we would expect to flow through the flow cell in the absence of any introduced dye. This was prepared by mixing the copper salt and organic linker solutions with an equal volume of ethanol, leaving for 60 minutes then centrifuging (1 min, 10,000 rpm, Eppendorf 5417R) and filtering.

*Batch synthesis*

For adsorption tests, batch-synthesised HKUST-1 was used. This was synthesised by mixing 10 mL of copper(II) nitrate hemipentahydrate (0.06 M in ethanol) and 10 mL of BTC (0.12 M in ethanol) which was subsequently left to mix at room temperature for 40 minutes. The reaction solution was subsequently used without any product isolation or workup. As such we could not record the yield, however we note that

*Offline analysis*

Prior to offline analysis, all samples were centrifuged (10,000 RPM, 1 min) in a microcentrifuge (Eppendorf 5417R). Offline absorbance measurements were carried out using a Shimadzu UV-2700 spectrophotometer. PXRD patterns were collected on a Bruker D2 Phaser using Cu Kα radiation source (λ = 1.5418 Å). SEM images were collected using a JEOL JSM7200F. 3D ED experiments were performed on a Rigaku Synergy-ED electron diffractometer ($LaB_6$, 200 kV), equipped with a Rigaku HyPix-ED hybrid pixel area array detector. Full details on 3D ED data collection and structure determination are given in the ESI. CCDC 2499142-2499143 contain the supplementary crystallographic data for this paper which can be obtained free of charge from the Cambridge Crystallographic Data Centre.[50] 3D ED raw data can be obtained at Zenodo.[51]

ACKNOWLEDGEMENTS

The authors acknowledge the University of Southampton's Faculty of Engineering & Physical Sciences (via the Centre of Excellence for Continuous Digital Chemical Engineering Science) for providing M.C.'s PhD studentship. D.N.R. and S.J.C. acknowledge the EPSRC for funding (EP/X014444/1 - A National Electron Diffraction Facility for Nanomaterial Structural Studies).

AUTHOR CONTRIBUTIONS

AMN and DB conceptualised the application-led analysis approach. MJC and JY developed the process technology. MJC conducted all experiments. MJC and DNR analysed the materials. MJC and AMN wrote the original manuscript. AMN, DB, SJC and DNR reviewed and edited the manuscript. AMN, DB and SJC acquired funding that supported the work.

Open Access Article. Published on 23 June 2026. Downloaded on 6/24/2026 4:50:44 AM.
This article is licensed under a Creative Commons Attribution 3.0 Unported Licence.

Journal of Materials Chemistry A Accepted Manuscript

View Article Online
DOI: 10.1039/D6TA03191A

Open Access Article. Published on 23 June 2026. Downloaded on 6/24/2026 4:50:44 AM.
This article is licensed under a Creative Commons Attribution 3.0 Unported Licence.

Journal of Materials Chemistry A Accepted Manuscript

## REFERENCES


1. H. Furukawa, K. E. Cordova, M. O'Keeffe and O. M. Yaghi, *Science*, 2013, **341**, 1230444.
2. C. Janiak and J. K. Vieth, *New Journal of Chemistry*, 2010, **34**, 2366–2388.
3. O. K. Farha, I. Eryazici, N. C. Jeong, B. G. Hauser, C. E. Wilmer, A. A. Sarjeant, R. Q. Snurr, S. T. Nguyen, A. Ö. Yazaydın and J. T. Hupp, *Journal of the American Chemical Society*, 2012, **134**, 15016–15021.
4. V. F. Yusuf, N. I. Malek and S. K. Kailasa, *ACS Omega*, 2022, **7**, 44507–44531.
5. X. Zhao, Y. Wang, D.-S. Li, X. Bu and P. Feng, *Advanced Materials*, 2018, **30**, 1705189.
6. A. Dhakshinamoorthy, Z. Li and H. Garcia, *Chemical Society Reviews*, 2018, **47**, 8134–8172.
7. H. D. Lawson, S. P. Walton and C. Chan, *ACS Applied Materials & Interfaces*, 2021, **13**, 7004–7020.
8. J. F. Olorunyomi, S. T. Geh, R. A. Caruso and C. M. Doherty, *Materials Horizons*, 2021, **8**, 2387–2419.
9. F. Yang, M. Du, K. Yin, Z. Qiu, J. Zhao, C. Liu, G. Zhang, Y. Gao and H. Pang, *Small*, 2022, **18**, 2105715.
10. J. Luczak, M. Kroczewska, M. Baluk, J. Sowik, P. Mazierski and A. Zaleska-Medynska, *Advances in Colloid and Interface Science*, 2023, **314**.
11. I. Thomas-Hillman, A. Laybourn, C. Dodds and S. Kingman, *Journal of Materials Chemistry A*, 2018, **6**, 11564–11581.
12. H. Al-Kutubi, J. Gascon, E. J. R. Sudhölter and L. Rassaei, *Chemelectrochem*, 2015, **2**, 462–474.
13. D. Chen, J. H. Zhao, P. F. Zhang and S. Dai, *Polyhedron*, 2019, **162**, 59–64.
14. C. Young, J. Wang, J. Kim, Y. Sugahara, J. Henzie and Y. Yamauchi, *Chemistry of Materials*, 2018, **30**, 3379–3386.
15. D. Chakraborty, A. Yurdusen, G. Mouchaham, F. Nouar and C. Serre, *Advanced Functional Materials*, 2024, **34**.
16. P. Dunne, E. Lester and R. Walton, *Reaction Chemistry & Engineering*, 2016, **1**, 352–360.
17. A. Adamo, R. L. Beingessner, M. Behnam, J. Chen, T. F. Jamison, K. F. Jensen, J.-C. M. Monbaliu, A. S. Myerson, E. M. Revalor, D. R. Snead, T. Stelzer, N. Weeranoppanant, S. Y. Wong and P. Zhang, *Science*, 2016, **352**, 61–67.
18. L. Capaldo, Z. Wen and T. Noël, *Chemical Science*, 2023, **14**, 4230–4247.
19. Z. Dong, Z. Wen, F. Zhao, S. Kuhn and T. Noël, *Chemical Engineering Science: X*, 2021, **10**, 100097.
20. B. J. Reizman and K. F. Jensen, *Accounts of Chemical Research*, 2016, **49**, 1786–1796.
21. R. Epps, K. Felton, C. Coley and M. Abolhasani, *Lab on a Chip*, 2017, **17**, 4040–4047.
22. I. Lignos, S. Stavrakis, G. Nedelcu, L. Protesescu, A. Demello and M. Kovalenko, *Nano Letters*, 2016, **16**, 1869–1877.
23. C. Mateos, M. J. Nieves-Remacha and J. A. Rincón, *Reaction Chemistry & Engineering*, 2019, **4**, 1536–1544.
24. R. W. Epps, M. S. Bowen, A. A. Volk, K. Abdel-Latif, S. Han, K. G. Reyes, A. Amassian and M. Abolhasani, *Advanced Materials*, 2020, **32**, 2001626.
25. A. M. Schweidtmann, A. D. Clayton, N. Holmes, E. Bradford, R. A. Bourne and A. A. Lapkin, *Chemical Engineering Journal*, 2018, **352**, 277–282.
26. B. Walker, J. Bannock, A. Nightingale and J. deMello, *Reaction Chemistry & Engineering*, 2017, **2**, 785–798.
27. D. Fabry, E. Sugiono and M. Rueping, *Reaction Chemistry & Engineering*, 2016, **1**, 129–133.
28. B. Reizman and K. Jensen, *Accounts of Chemical Research*, 2016, **49**, 1786–1796.

View Article Online
DOI: 10.1039/D6TA03191A

29. B. He, L. K. Macreadie, J. Gardiner, S. G. Telfer and M. R. Hill, *Acs Applied Materials & Interfaces*, 2021, **13**, 54284–54293.
30. M. Taddei, N. Casati, D. A. Steitz, K. C. Dümbgen, J. A. van Bokhoven and M. Ranocchiari, *Crystengcomm*, 2017, **19**, 3206–3214.
31. F. Ahmadijokani, A. Ghaffarkhah, H. Molavi, S. Dutta, Y. Lu, S. Wuttke, M. Kamkar, O. Rojas and M. Arjmand, *Advanced Functional Materials*, 2024, **34**.
32. X. Liu, Y. Shan, S. Zhang, Q. Kong and H. Pang, *Green Energy & Environment*, 2023, **8**, 698–721.
33. M. Mon, R. Bruno, J. Ferrando-Soria, D. Armentano and E. Pardo, *Journal of Materials Chemistry A*, 2018, **6**, 4912–4947.
34. L. Huelsenbeck, H. Luo, P. Verma, J. Dane, R. Ho, E. Beyer, H. Hall, G. M. Geise and G. Giri, *Crystal Growth & Design*, 2020, **20**, 6787–6795.
35. M. Faustini, J. Kim, G. Y. Jeong, J. Y. Kim, H. R. Moon, W. S. Ahn and D. P. Kim, *Journal of the American Chemical Society*, 2013, **135**, 14619–14626.
36. C. McKinstry, E. J. Cussen, A. J. Fletcher, S. V. Patwardhan and J. Sefcik, *Chemical Engineering Journal*, 2017, **326**, 570–577.
37. M. Rubio-Martinez, M. P. Batten, A. Polyzos, K.-C. Carey, J. I. Mardel, K.-S. Lim and M. R. Hill, *Scientific Reports*, 2014, **4**, 5443.
38. J. C. Shen, X. Z. Wang, L. M. Zhang, Z. Yang, W. B. Yang, Z. Q. Tian, J. Q. Chen and T. Tao, *Journal of Cleaner Production*, 2018, **184**, 949–958.
39. K. S. Lin, A. K. Adhikari, C. N. Ku, C. L. Chiang and H. Kuo, *International Journal of Hydrogen Energy*, 2012, **37**, 13865–13871.
40. G. Majano, O. Martin, M. Hammes, S. Smeets, C. Baerlocher and J. Pérez-Ramírez, *Advanced Functional Materials*, 2014, **24**, 3855–3865.
41. S. Lin, Z. L. Song, G. B. Che, A. Ren, P. Li, C. B. Liu and J. H. Zhang, *Microporous and Mesoporous Materials*, 2014, **193**, 27–34.
42. R. Sabouni, A. Aidan, A. AlObeidli, F. Lahib, H. H. Bacha, R. Kassermally and S. Jarmakani, *Desalination and Water Treatment*, 2019, **138**, 301–312.
43. C. Rodríguez-Esteban, R. Ayala and C. López-Cartes, *Journal of Solid State Chemistry*, 2024, **339**.
44. S. Roy, J. Darabdhara and M. Ahmaruzzaman, *Journal of Hazardous Materials Letters*, 2024, **5**.
45. Y. Han, I. Borne, B. Dutta, R. Clowes, H. Qu, A. James, C. E. Boott, M. A. Little and A. I. Cooper, *Angewandte Chemie International Edition*, 2025, **64**, e202510400.
46. S. L. Griffin, M. L. Briuglia, J. H. ter Horst and R. S. Forgan, *Chemistry – A European Journal*, 2020, **26**, 6910–6918.
47. F. Massingberd-Mundy, S. Poulston, S. Bennett, H. H.-M. Yeung and T. Johnson, *Scientific Reports*, 2020, **10**, 17355.
48. C. Taylor, A. Pomberger, K. Felton, R. Grainger, M. Barecka, T. Chamberlain, R. Bourne, C. Johnson and A. Lapkin, *Chemical Reviews*, 2023, **123**, 3089–3126.
49. M. A. Morin, W. Zhang, D. Mallik and M. G. Organ, *Angewandte Chemie International Edition*, 2021, **60**, 20606–20626.
50. Cambridge Crystallographic Data Centre, www.ccdc.cam.ac.uk/structures).
51. Zenodo, https://www.doi.org/10.5281/zenodo.17484900).

Open Access Article. Published on 23 June 2026. Downloaded on 6/24/2026 4:50:44 AM.
This article is licensed under a Creative Commons Attribution 3.0 Unported Licence.

Journal of Materials Chemistry A Accepted Manuscript

Crystallographic data is available via CCDC (see details in Methods section and ESI).

View Article Online
DOI: 10.1039/D6TA03191A

Open Access Article. Published on 23 June 2026. Downloaded on 6/24/2026 4:50:44 AM.
This article is licensed under a Creative Commons Attribution 3.0 Unported Licence.

Journal of Materials Chemistry A Accepted Manuscript